Available online at www.sciencedirect.com
ScienceDirect
Journal of Power Sources 173 (2007) 990–997
JOURNAL OF POWER SOURCES
www.elsevier.com/locate/jpowsour

Calendar life study of Li-ion pouch cells

Qi Zhang, Ralph E. White *

Center for Electrochemical Engineering, Department of Chemical Engineering, University of South Carolina, Columbia, SC 29208, USA

Received 29 June 2007; received in revised form 10 August 2007; accepted 13 August 2007
Available online 24 August 2007

Abstract

A calendar life study was conducted on lithium ion pouch cells which were stored under float charge condition at five temperatures. The half cell study showed that the anode experienced severe loss of the active material, especially at high temperatures. The capacity fade mechanisms were then proposed. The capacity fade at low temperatures could mostly be caused by the loss of lithium inventory to side reactions and impedance increase. The capacity fade at high temperatures demonstrated a two-regime pattern. The fading mechanisms in the first regime could be similar to those at low temperatures. The capacity fade in the second regime could be dominated by the severe loss of active carbon material. The impedance rise plays a minor role in the second capacity fade regime.

Keywords: Calendar life study; Capacity fade; Loss of active carbon

1. Introduction

The calendar life of lithium ion batteries is an important factor in the evaluation of their dependability, stability and cost. The calendar life study defined in the PNGV battery test manual [1] is designed to evaluate the cell degradation as a result of the passage of time with minimal usage. Several national labs and groups [2–9] have studied the storage of lithium ion batteries. For example, Broussely et al. [2] concluded that lithium oxidation on the negative electrode is a major side reaction affecting the cell capacity on storage at high temperatures. Wright et al. [5] observed a square root of time dependence of the cell resistance after long time storage. Asakura et al. [7] observed that a 15 °C increase in temperature and 0.1 V increase in charging voltage could cut the cell life in half under floating charge conditions.

In this work, the capacity fade of lithium ion pouch cells was studied under float charge condition at different temperatures. Half cell studies on the used electrodes were conducted to understand more about the capacity fade of these cells. The capacity fade mechanisms were then proposed and discussed based on the findings from the full cell tests and half cell studies.

2. Experiments

Ten lithium ion pouch cells received from Nation Reconnaissance Office were used in the calendar life study. Each cell consisted of four (double-sided) positive electrodes and five (three double-sided and two single-sided) negative electrodes. The active material of the positive and negative electrode is $LiCoO_2$ and carbon (mesocarbon micro-bead), respectively. One molar $LiPF_6$ in a quaternary solvent mixture of EC, PC, EMC and DEC was used as the electrolyte. The double-sided positive electrodes were contained in bags made with separators. Three double-sided negative electrodes were sandwiched between four positive electrodes, while the two single-sided negative electrodes covered the outer positive electrodes. The entire assembly of anodes, cathodes and separators were enclosed by proprietary material to make a pouch cell. The pouch cells were vacuum degassed and mechanically clamped between two aluminum plates (for each cell) when they were shipped to our lab. The name plate capacity of these cells was 1.656 Ah and the experiment charge and discharge C rate currents were determined based on the nameplate capacity of the cell ($C = 1.656$ A).

The cells were stored at five different temperatures: 5, 15, 25, 35, and 45 °C. The test procedures and the sequence were summarized in Fig. 1. The procedures consisted of rate capability test, storage at float charge condition and monthly capacity

* Corresponding author. Tel.: +1 803 777 3270; fax: +1 803 777 6769.
E-mail address: white@engr.sc.edu (R.E. White).

0378-7753/$ – see front matter © 2007 Elsevier B.V. All rights reserved.
doi:10.1016/j.jpowsour.2007.08.044

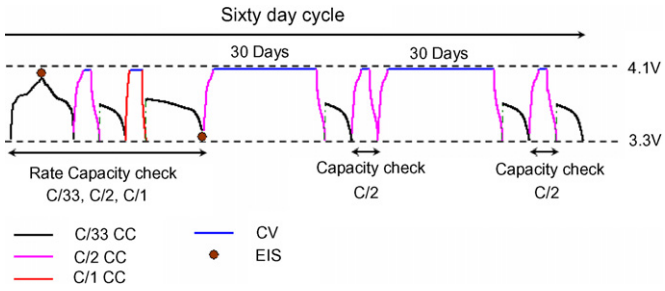

Fig. 1. Test procedures for the calendar life study.

check. The sequence was rate capability test, storage for 30 days, capacity check, storage for 30 days and capacity check. After one sequence was finished, another sequence would start with the rate capacity test. The designed procedures would be helpful to build a model from the experiment data. That is, the data from the rate capability tests could be used to formulate the model while the data from the monthly capacity checks could be used to validate the model. In the rate capability tests, three current rates were used to evaluate the performance of the cells. They were *C*/33, *C*/2 and *C*/1 rates. At *C*/33 rate, a constant current (CC) protocol was used to charge and discharge the cells. At *C*/2 and *C*/1 rates, CC–CV (constant voltage) protocol was used to charge the cells. A two stage CC protocol was used to discharge the cells, that is, *C*/2 or *C*/1 rate followed by *C*/33 rate. The voltage window for the rate capability tests was 3.3–4.1 V. Electrochemical impedance spectroscopy (EIS) measurements were also taken at the end of the rate capability tests. The frequency range for the impedance measurement was 10 kHz to 0.1 Hz and the amplitude of the input signal was 10 mV. The rate capability tests and EIS measurements were both performed at the storage temperatures. During storage, the cells were stored under a trickle charge condition to maintain the cell potential at 4.1 V. All the experiments were done in the Tenney environment chambers and the battery testing hardware was the Arbin BT-2000 testing system. The data were collected using the MitsPro software provided by Arbin.

Half cell studies were performed on the used electrodes harvested from the aged cells to understand the capacity fade in individual electrodes. The residual capacity and the intrinsic capacity of used electrodes were measured. One pouch cell from each temperature was first discharge to 3.0 V at room temperature with a small current to ensure a complete discharge. Then they were opened inside an argon filled glove box. Carbon disc electrodes of diameter 5/8 in. were punched out of the single-sided carbon electrode sheets inside the glove box to prevent any possible reactions of lithiated carbon with air. For the double-sided $LiCoO_2$ cathodes, one side of the electrode coating was scratched off the current collector plate by hand outside the glove box before they were used to make disc electrodes of diameter 5/8 in. Coin cells of type CR2025 were made with $LiCoO_2$ or carbon disc electrode as working electrode and lithium foil as counter electrode. The $LiCoO_2$ coin cells were first discharged to 2.0 V to measure the residual capacities. Another charge and discharge cycle between the voltage window 2.0–4.3 V measured the intrinsic (reversible) capacities of the $LiCoO_2$ coin cells. The carbon coin cells were first charged to 2.0 V to measure the residual capacities. Another discharge and charge cycle between the voltage window 0.01–2.0 V measured the intrinsic capacities of the carbon coin cells.

3. Results and discussion

3.1. Calendar life data

The pouch cells stored at 5, 15 and 25 °C were tested for 18 months. At the end of the calendar life study, they had a capacity fade percentage of around 17%, 20% and 62%, respectively. The cells stored at 35 and 45 °C were tested for 14 and 10 months, respectively. The capacity fade percentage of the cells reached more than 90% at the end of storage test.

The discharge capacities measured at *C*/33 rate in the rate capability tests are presented in Fig. 2. Because of the small current used, the impedance effect would be minimized and the measured discharge capacities reflect the true cell capacities. The capacity fade at low temperatures is mostly linear with time, but nonlinear at high temperatures. Cells stored at high temperatures experience an accelerated capacity fade after a few months of storage. When they approach the end of life, the capacity fade slows down. The pattern is consistent with the results found in a previous study [8] where cells are stored at 35 °C under both float charge condition and open circuit condition.

Three different current rates were used in the bi-monthly rate capability tests to measure the cell performance. The discharge capacities at different current rates are presented in Fig. 3 for selected temperatures. The capacities measured at high rates appear to fade in a similar pattern as those measured at low rates. However, a close examination of these experimental data reveals that the capacity fade mechanisms could be different for different temperatures. A detailed discussion on possible capacity fade mechanisms is presented in Section 3.3.

Fig. 4 compares the pre-monthly and monthly cell capacities measured at *C*/2 rate at different temperatures. A two stage

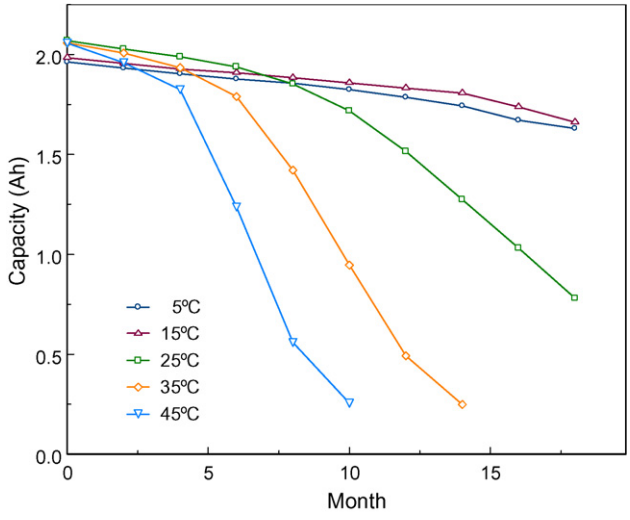

Fig. 2. Capacity fade at *C*/33 rates for different temperatures.

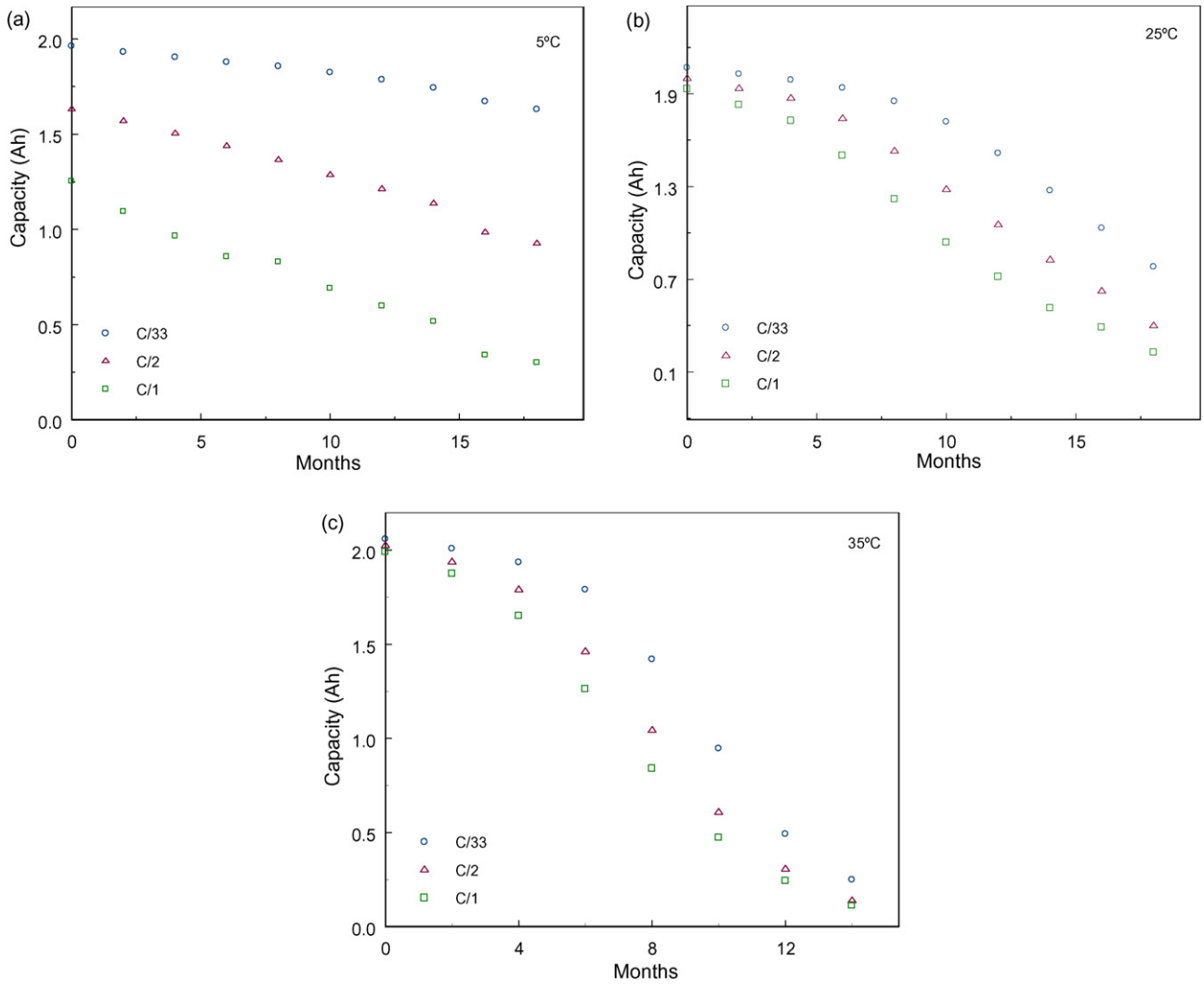

Fig. 3. Discharge capacities measured at different current rates for selected temperatures.

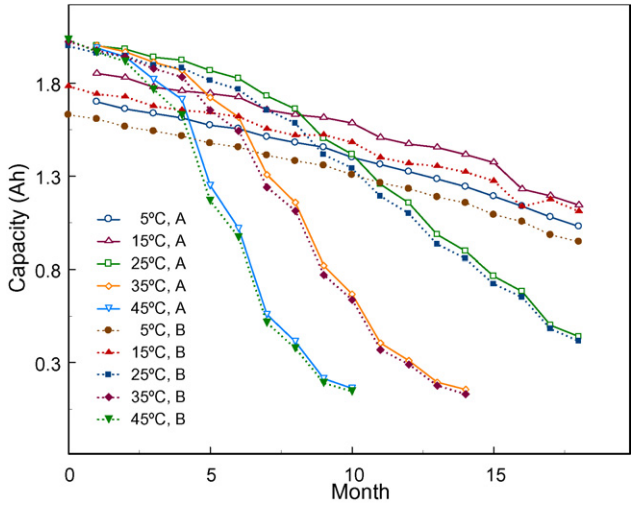

Fig. 4. The pre-monthly (A, hollow markers) and monthly (B, solid markers) discharge capacities measured at *C*/2 rate.

CC protocol (*C*/2 + *C*/33) is used to fully discharge the cells from float charge condition before the monthly capacity check is performed. The capacity measured in this step is called the pre-monthly capacity. The pre-monthly capacities are slightly higher than the monthly capacities, especially at low temperatures. This is because the cells were trickle charged during storage. Thus they are close to an equilibrium condition at 4.1 V and could delivered more capacity after storage (under float condition).

The increase of cell impedance with storage time is shown in Fig. 5 for selected temperatures. Two semicircles can be identified from the impedance plots. The first semicircle in the high to medium frequency range can be attributed to the surface film around the particles and the second semicircle in the low frequency range can be attributed to the charge transfer process. The low frequency semicircles become markedly large as storage time increases, while the high frequency ones become a little bit larger. Undesirable side reactions could happen during the storage at float charge condition. The deposition of side reaction products on the particle surface could lead to a more sluggish charge transfer process as shown in the figure.

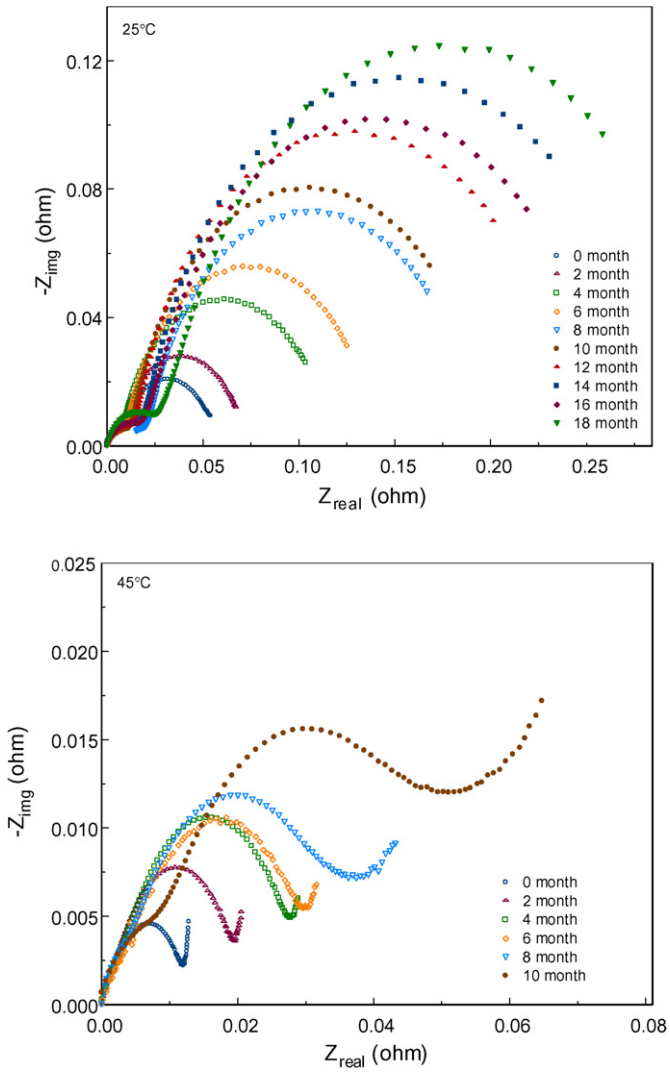

Fig. 5. The increase of cell impedance with storage time at selected temperatures.

3.2. Half cell study

To understand more about the rapid capacity fade of these pouch cells, half cell study was performed on the used electrodes. The residual and intrinsic capacities were measured in the half cell study.

The residual capacity of a $LiCoO_2$ electrode is the amount of empty sites left in the CoO_2 framework when a full cell is fully discharged. The $LiCoO_2$ electrode is the only source for cyclable lithium ions in a full cell. When lithium ions are irreversibly consumed in the side reactions, there would not be enough cyclable lithium ions available in the system to intercalate the $LiCoO_2$ electrode back to its original state. Thus the $LiCoO_2$ electrode gradually becomes less intercalated and accrues a residual capacity. For the carbon electrode, the residual capacity is the amount of lithium ions left in the electrode. The carbon electrode could become less discharged under increased cell impedance and accumulate a residual capacity.

The intrinsic (reversible) capacity of an electrode is the total amount of active material in the electrode. The $LiCoO_2$ electrode could lose active material (intrinsic capacity) due to cobalt dissolution, loss of electronic conductivity within the electrode by segregation between active particles or swelling of the binder, etc. The carbon electrode could lose active material because of carbon exfoliation, the isolation of carbon particles by continuous SEI formation and/or the mechanical failure of the anode.

Table 1
The residual and intrinsic capacity of the $LiCoO_2$ coin cells[a]

	$LiCoO_2$			
	Residual capacity (mAh)	Residual percentage[b]	Intrinsic capacity (mAh)	Intrinsic percentage[c]
Fresh			6.17	
5 °C	0.626	10.7	5.87	95.6
15 °C	0.647	11.6	5.56	91.6
25 °C	2.792	48.3	5.78	93.5
35 °C	3.287	60.6	5.43	89.3
45 °C	2.317	51.3	4.52	74.2

The cells stored at 5, 15 and 25 °C have a capacity fade percentage of 16%, 20% and 62%, respectively and a storage time of 18 months. The cell stored at 35 and 45 °C has a capacity fade percentage of more than 90% and a storage time of 14 and 10 months, respectively.

[a] 5/8 in. disc electrode in a coin cell.

[b] The residual percentage is calculated as (residual/intrinsic) × 100.

[c] The intrinsic percentage is calculated as (intrinsic/intrinsic(fresh)) × 100.

Table 1 compares the intrinsic capacities of the $LiCoO_2$ coin cells made from used $LiCoO_2$ electrodes. The intrinsic capacities of the used $LiCoO_2$ electrodes stored at 5–35 °C are close to each other even though the capacity fade percentages of the cells are significantly different. The intrinsic capacity for the electrode stored at 45 °C is much smaller than that at 35 °C even though they have similar capacity fade percentage. The half cell study indicates that the loss of intrinsic capacity in the $LiCoO_2$ electrode is not directly proportional to the capacity fade of the full cell. High temperature (45 °C) is more influential to the loss of active cathode material.

The residual capacities of the $LiCoO_2$ coin cells are also compared in Table 1. The residual capacities increase mostly with the capacity fade percentages. This is because high capacity fade percentage indicates that more lithium ions are lost during storage, thus more empty sites left in the $LiCoO_2$ electrode.

Fig. 6 compares the low rate discharge profiles and dQ/dV plots for the $LiCoO_2$ coin cells. The voltage ripples in the discharge profiles and the peaks in the dQ/dV plots at around 4.1 V become flat for the electrodes stored at high temperatures, which could be due to a loss of electronic conductivity within the electrode.

Table 2 compares the intrinsic and residual capacities of the carbon coin cells. The aged carbon electrodes have increased residual capacities at elevated temperatures. The intrinsic capacity data indicate that the anode experienced a severe loss of active carbon material, especially at high temperatures, which could be a significant factor for the capacity fade. The severe carbon loss could result from the mechanical failure of the anode, where the carbon particles lose contact with the electrode.

The severe carbon loss could contribute to the cell capacity fade in several ways. First, the anode is mostly kept in

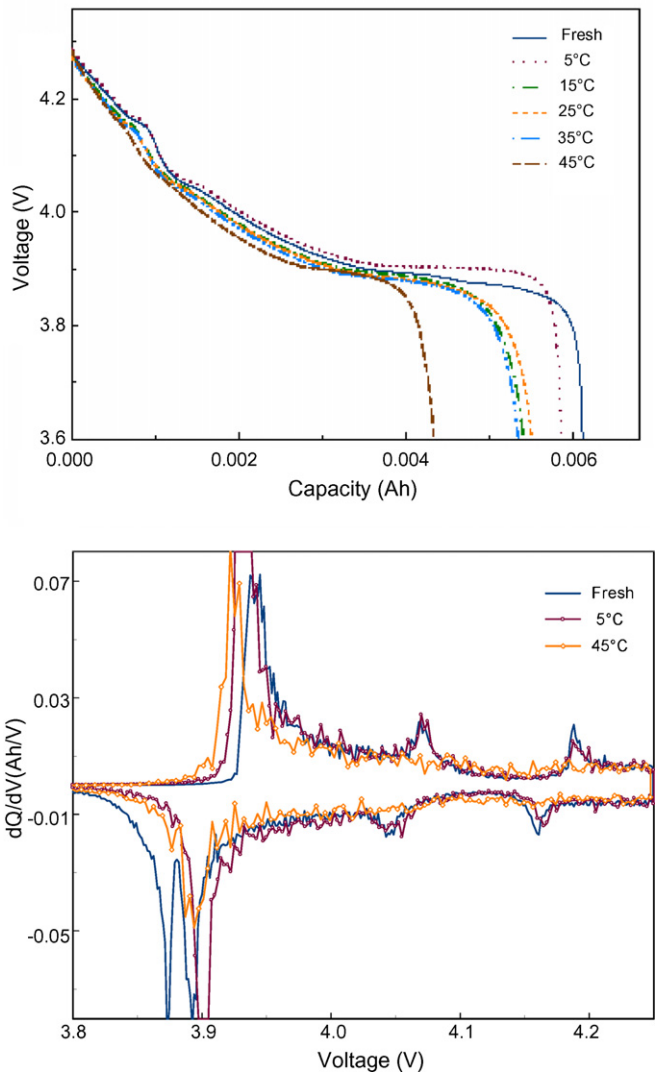

Fig. 6. Discharge profiles and the dQ/dV profiles of the $LiCoO_2$ coin cells made with aged $LiCoO_2$ electrode.

charged/lithiated state during storage (float charge). The subsequent isolation of lithiated carbon particles would trap those lithium ions inside, thus directly expedite the loss of cyclable lithium ions. Second, as the anode loses active carbon, it also loses the electro-active surface area for the insertion reaction. The same discharge current means a higher current density (current/electro-active area in A cm^{-2}) for an aged carbon electrode, which would cause increased overpotential on the anode. Third, the severe carbon loss could disturb the capacity ratio between the anode and the cathode. The fresh carbon electrode in a pouch cell has an intrinsic capacity of 2.5 Ah. About 80% of that capacity is used as the discharge capacity of a fresh cell could reach about 2.0 Ah. However, the aged carbon electrode stored at 45 °C has only 0.25 Ah capacity left which is close to the discharge capacity of the full cell before opening. Thus, the deposition of lithium on the anode could happen during storage. The claim is also supported by the observation that the surfaces of used carbon electrodes stored at high temperatures were entirely covered by white products which are highly reactive with air to release gas.

Fig. 7 shows the low rate discharge profiles and the dQ/dV plots for the used carbon electrodes. The voltage plateaus are well distinguishable in those discharge profiles. The flatting of peaks in the dQ/dV plots could be caused by the loss of conductivity because of surface film formation and impedance rise inside the electrode.

3.3. Capacity fade mechanism

Our half cell study reveals that the used carbon electrodes experienced severe loss of active material after storage at high temperatures. Nevertheless, how the severe carbon loss contributes to the capacity fade of the pouch cells is not clear. In the following section, we would re-examine some experiment data from the full cell study and discuss in detail the possible capacity fade mechanisms for the pouch cells.

The discharge capacities under different current rates at 5 °C have been presented in Fig. 3a. The capacity fade is mostly linear for all three current rates. Thus dotted lines are added to the figure which is re-plotted as Fig. 8.

An apparent observation of Fig. 8 (5 °C) is that the capacity fade rates at C/1 and C/2 rates, as indicated by the slopes of the dotted lines, are higher than that at C/33 rates. This behavior could usually be attributed to the increase of cell impedance. The half cell study shows that the active material losses in both the anode and the cathode are small at low temperatures. Therefore,

Table 2
The residual and intrinsic capacity of the carbon coin cells[a]

	Carbon[a]					
	Residual capacity (mAh)	Residual percentage	Intrinsic capacity (mAh)	Intrinsic percentage	Electrode capacity[b] (Ah)	Cell capacity[c] (Ah)
Fresh			5.61		2.49	2.05
5 °C	0.074	1.64	4.5	80.2	1.99	1.63
15 °C	0.11	2.66	4.14	73.8	1.84	1.66
25 °C	0.46	22.8	2.02	36.0	0.90	0.78
35 °C	0.45	42.5	1.06	18.9	0.47	0.25
45 °C	0.13	23.2	0.56	9.98	0.25	0.25

[a] 5/8 in. disc carbon electrode (1.98 cm^2) in a coin cell.
[b] Capacity of the carbon electrode (877.74 cm^2) in a full cell. The capacity is calculated using (intrinsic capacity/1.98 × 877.74).
[c] Discharge capacities (at C/33 rate) of a full cell at the end of the storage test.

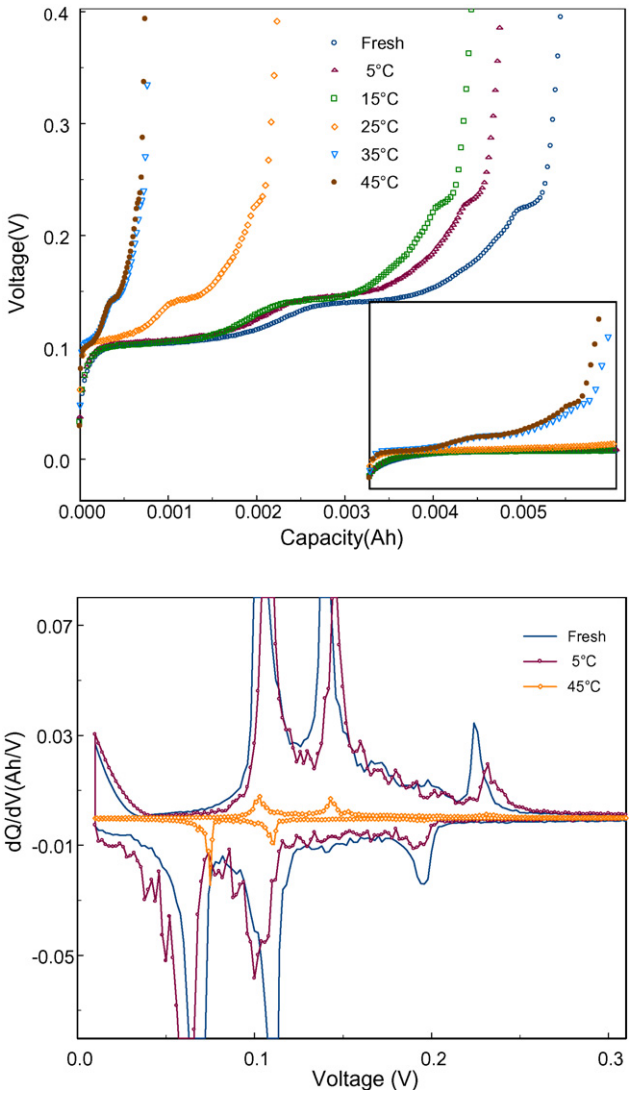

Fig. 7. Discharge profiles and the dQ/dV profiles of the carbon coin cells made with aged carbon electrode.

it is proposed that the major capacity fade mechanisms at low temperature such as 5 °C could be loss of Li^+ inventory to side reactions and the increase of cell impedance. The capacity fade measured at low C/33 rate is caused mostly by the loss of cyclable Li^+s to side reactions. The increase of cell impedance is less important at low current rates. The accelerated capacity fade at C/1 and C/2 rates is caused by the combined effect of loss of Li^+ inventory and impedance increase.

Fig. 3b compares the discharge capacities at 25 °C. A close examination of the data reveals that the capacity fade at 25 °C could be regarded as two fading regimes (mostly linear) in sequence, instead of as one nonlinear regime. Dotted lines are added to the figure which is re-plotted as Fig. 9 to illustrate the two-regime concept. The two capacity fade regimes suggest that the controlling capacity fade mechanisms could be different for the two regimes.

An important observation of Fig. 9 is that the capacity fade rates at C/1 and C/2 rates are NOT always higher than that at low C/33 rate. They are higher in the first few (6) months storage

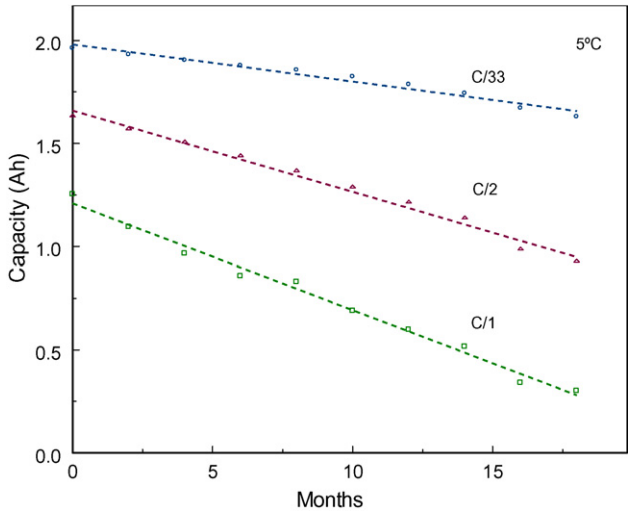

Fig. 8. Capacity fade at 5 °C. The capacity fade mechanisms could be Li^+ consuming side reactions and the increase of cell impedance. The capacity fade rates at C/2 and C/1 rates (indicated by the slopes of the dotted lines) are higher than that at C/33 rate because of increased cell impedance.

period, similar to what Fig. 8 shows for 5 °C. Then they largely equal to the capacity fade rate at C/33 rate as the dotted lines run mostly parallel to each other. The observation suggests that the dominating capacity fade mechanisms for the second capacity fade regime could have overwhelmed the effect of increased cell impedance.

Bloom et al. [10,11] also observed a two-regime pattern for the increase of area specific impedance (ASI) and capacity fade at C/1 rate which is largely attributed to the ASI increase. The proposed mechanism for ASI increase is that side reactions change from diffusion control to surface reaction control

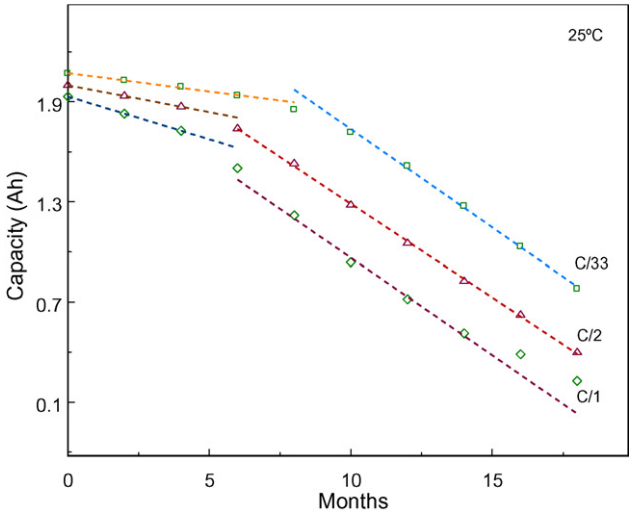

Fig. 9. Capacity fade at 25 °C. There could be two capacity fade regimes for cells stored at 25 °C. The capacity fade in the first fading regime is mostly caused by loss of lithium inventory to side reactions and impedance increase, the same as at 5 °C. The dominating mechanism for the second regime could be the severe loss of active carbon in the anode. The impedance rise plays a minor role in the second regime because the capacity fade rates at C/1 and C/2 rates are mostly the same as that at C/33 rate.

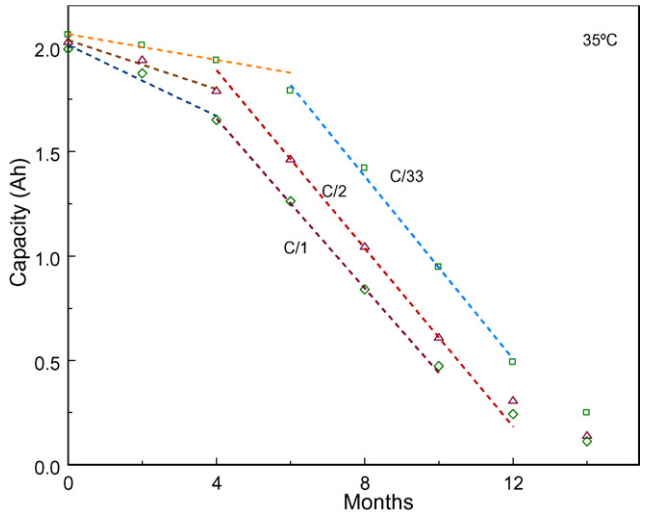

Fig. 10. Capacity fade at 35 °C. The capacity fade pattern and mechanisms at 35 °C are similar to those at 25 °C.

[11]. However, their mechanism does not apply to our calendar life study. If the impedance rise still plays a major role in our second fading regime, the capacity fade rates at *C*/1 and *C*/2 rates should be higher than that at *C*/33 rate, as in Fig. 8.

Hereby the capacity fade mechanisms are proposed for the cells stored at 25 °C. During the first few months storage period at 25 °C (the first fade regime), the major mechanisms are loss of Li^+ inventory and increase of cell impedance. Thus the capacity fade in this regime resembles a similar pattern as at 5 °C. Then in the second fade regime, the capacity fade becomes dominated by the loss of active carbon materials. It should be noted that the loss of active carbon could also cause loss of lithium inventory in our calendar life study, because the anode is mostly in charged/lithiated state (float charged in storage). The impedance rise appears to be a minor fading mechanism in the second regime based on the discussion in previous paragraphs.

For cells stored at high temperatures such as 35 and 45 °C, similar capacity fade patterns are observed. For example, Fig. 10 illustrates the two fading regime pattern for the cell stored at 35 °C. The capacity fade in the first regime could be caused by loss of lithium inventory and impedance rise. The capacity fade in the second regime is dominated by the severe loss of active carbon in the anode. The transition from the first fading regime to the second one occurs early at high temperatures as the anode is under more stress at high temperatures. The electrolyte decomposition could also have contributed to the cell capacity fade at high temperatures. The vacuum-degassed pouch cells were found to have signs of inflation at the end of storage test at 35 and 45 °C. Leakage was observed around the seal near the electrode tabs for cells stored at 45 °C.

4. Conclusions

A calendar life study was conducted on lithium ion pouch cells containing $LiCoO_2$ as the cathode and carbon as the anode. The cells were stored at float charge condition at five different temperatures. The capacity fade appears to be linear with time at low temperatures, but nonlinear at high temperatures.

Half cell studies showed that the $LiCoO_2$ electrode retained most of the intrinsic capacity, except at 45 °C. However, the anode experienced a severe loss of active carbon during storage, especially at high temperatures (60% for 25 °C, over 80% for 35 and 45 °C, Table 2). The severe carbon loss could be caused by the isolation of carbon particles by the mechanical failure of the anode.

The severe carbon loss could contribute to the cell capacity fade by trapping Li^+s inside isolated carbon particles (lithiated in float charge condition), reducing the electro-active surface area and disturbing the anode/cathode capacity ratio. The analysis showed that deposition of lithium on the anode could happen during float charge. This is directly supported by the observation that the aged carbon electrodes at high temperatures were covered entirely with white products which are highly reactive with air to release gas.

The capacity fade mechanisms for the calendar life study are then proposed based on the findings from the full cell testing and half cell study. The capacity fade at low temperatures is mostly caused by the loss of lithium inventory to side reactions and impedance rise.

The capacity fade at high temperatures demonstrates a two-regime fading pattern. The fading mechanisms in the first regime are mostly Li^+ loss and impedance rise, similar as those at low temperatures. The capacity fade in the second regime could be dominated by the severe loss of active carbon. The impedance rise might play a minor role as the experiment data show that the capacity fade rates at *C*/2 and *C*/1 rates are almost the same as that at *C*/33 rate in the second regime.

Acknowledgement

The authors would like to acknowledge the financial support by the National Reconnaissance Office (NRO) under the contract # NRO-000-03-C-0122 for this project.

References

[1] PNGV Test Plan for ATD 18650 Gen 1 Lithium-Ion Cells, Revision 4, EHV-TP-103, December 1999.
[2] M. Broussely, S. Herreyre, P. Biensan, P. Kasztejna, K. Nechev, R.J. Staniewicz, J. Power Sources 97/98 (2001) 13.
[3] K. Ammine, C.H. Chen, J. Liu, M. Hammond, A. Jansen, D. Dees, I. Bloom, D. Vissers, G. Henriksen, J. Power Sources 97/98 (2001) 684.
[4] I. Bloom, B.W. Cole, J.J. Sohn, S.A. Jones, E.G. Polzin, V.S. Battaglia, G.L. Henriksen, C. Motloch, R. Richardson, T. Unkelhaeuser, D. Ingersoll, H.L. Case, J. Power Sources 101 (2001) 238.
[5] R.B. Wright, C.G. Motloch, J.R. Belt, J.P. Christophersen, C.D. Ho, R.A. Richardson, I. Bloom, S.A. Jones, V.S. Battaglia, G.L. Henriksen, T. Unkelhaeuser, D. Ingersoll, H.L. Case, S.A. Rogers, R.A. Sutula, J. Power Sources 110 (2002) 445.
[6] D.P. Abraham, J. Liu, C.H. Chen, Y.E. Hyung, M. Stoll, N. Elsen, S. Maclaren, R. Twesten, R. Haasch, E. Sammann, I. Petrov, K. Amine, G. Henriksen, J. Power Sources 119–121 (2003) 511.

[7] K. Asakura, M. Shimomura, T. Shodai, J. Power Sources 119–121 (2003) 902.
[8] R.P. Pamasamy, R.E. White, B.N. Popov, J. Power Sources 141 (2005) 298.
[9] K. Kumaresan, Q. Guo, P. Ramadass, R.E. White, J. Power Sources 158 (2006) 679.
[10] I. Bloom, B.G. Potter, C.S. Johnson, K.L. Gering, J.P. Christophersen, J. Power Sources 155 (2006) 415.
[11] I. Bloom, S.A. Jones, V.S. Battaglia, G.L. Henriksen, J.P. Christophersen, R.B. Wright, C.D. Ho, J.R. Belt, C.G. Motloch, J. Power Sources 124 (2003) 538.